

Submitted to Journal of
Chemical Physics

RECEIVED
LAWRENCE
RADIATION LABORATORY

UCRL-20550
Preprint

CS

DOCUMENTS SECTION

MOLECULAR ORBITAL CORRELATIONS AND
ION-MOLECULE REACTION DYNAMICS

Bruce H. Mahan

March 1971

AEC Contract No. W-7405-eng-48

TWO-WEEK LOAN COPY

*This is a Library Circulating Copy
which may be borrowed for two weeks.
For a personal retention copy, call
Tech. Info. Division, Ext. 5545*

LAWRENCE RADIATION LABORATORY
UNIVERSITY of CALIFORNIA BERKELEY

UCRL-20550

CS

DISCLAIMER

This document was prepared as an account of work sponsored by the United States Government. While this document is believed to contain correct information, neither the United States Government nor any agency thereof, nor the Regents of the University of California, nor any of their employees, makes any warranty, express or implied, or assumes any legal responsibility for the accuracy, completeness, or usefulness of any information, apparatus, product, or process disclosed, or represents that its use would not infringe privately owned rights. Reference herein to any specific commercial product, process, or service by its trade name, trademark, manufacturer, or otherwise, does not necessarily constitute or imply its endorsement, recommendation, or favoring by the United States Government or any agency thereof, or the Regents of the University of California. The views and opinions of authors expressed herein do not necessarily state or reflect those of the United States Government or any agency thereof or the Regents of the University of California.

MOLECULAR ORBITAL CORRELATIONS AND ION-MOLECULE REACTION DYNAMICS

Bruce H. Mahan

Department of Chemistry and Inorganic Materials Research
Division of the Lawrence Radiation Laboratory,
University of California, Berkeley, California

We examine the application of molecular orbital correlation diagrams to ion-molecule collision processes. In situations where the reactant and product orbitals are few in number and well spaced in energy, the correlation diagrams give a clear picture of how the reactant electron configuration evolves to that of the products. The diagrams lead to a simple explanation of why the endothermic $\text{H}_2^+(\text{He},\text{H})\text{HeH}^+$ and $\text{H}_2^+(\text{Ne},\text{H})\text{NeH}^+$ reactions occur, whereas the exothermic processes $\text{He}^+(\text{H}_2,\text{H})\text{HeH}^+$ and $\text{Ne}^+(\text{H}_2,\text{H})\text{NeH}^+$ have undetectably small cross sections. Similarly, it is possible to use the diagrams to explain why the $\text{CO}^+(\text{H}_2,\text{H})\text{HCO}^+$ and $\text{N}_2^+(\text{H}_2,\text{H})\text{N}_2\text{H}^+$ reactions proceed by direct interaction mechanisms despite the substantial stability of the intermediate ions H_2CO^+ and N_2H_2^+ . Several other applications of the diagrams are discussed.

In recent years, much experimental evidence concerning the nature of gaseous ion-molecule reactions has been obtained. While the origin of the sometimes spectacularly large cross sections of these reactions is understood, a number of other phenomena have been discovered that so far have had no clear, generally accepted explanation. For example, the reaction of H_2^+ with He to form HeH^+ and H is a well-known,^{1,2} slightly endothermic reaction which has a substantial cross section at kinetic energies above threshold. However, the corresponding strongly exothermic reaction between He^+ and H_2 does not occur. The analogous situation holds for the $(\text{Ne}-\text{H}_2)^+$ system.^{2,3} In contrast, for $(\text{Ar}-\text{H}_2)^+$ and $(\text{Kr}-\text{H}_2)^+$, formation of the rare gas hydrides occurs⁴ regardless of where the charge initially resides.

Another apparently puzzling set of phenomena is the observation^{5,6} that the $\text{N}_2^+(\text{H}_2, \text{H})\text{N}_2\text{H}^+$ and $\text{CO}^+(\text{H}_2, \text{H})\text{HCO}^+$ reactions proceed by direct, impulsive interactions, rather than through persistent complexes, even at low relative kinetic energies. The intermediate ions N_2H_2^+ and H_2CO^+ formed by electron impact are well known⁷ to be stable. Their stability makes it clear that the potential energy surfaces for these systems have the deep wells which should make the effects of persistent complexes appear in the product angular distributions. In fact, a persistent complex has been detected⁸ in the highly analogous $\text{O}_2^+(\text{H}_2, \text{H})\text{HO}_2^+$ reaction, and this makes it even less clear why the reactions of N_2^+ and CO^+ with H_2 proceed by an impulsive mechanism.

The answer to these questions lies, of course, in consideration of the detailed potential energy surfaces for the reactions. However, these surfaces are not yet available, and may be obtained for polyatomic systems only after the expenditure of considerable cost and effort. In the meantime, interpretation of scattering and rate data must be based on qualitative features of the potential energy surfaces discerned by approximate methods.

The most obvious feature common to the surfaces for ion-molecule reactions is the strong, long-range attraction which arises from the dipole moment induced in a polarizable molecule by the approaching ion. This ion-induced dipole interaction potential varies as $-\alpha e^2/(2r^4)$, where α is the molecular polarizability, e is the electronic charge, and r is the ion-molecule separation. This potential has been used successfully and probably correctly to rationalize the magnitude and energy dependence of the cross sections of many ion-molecule reactions in the limit of low relative kinetic energies of collision.⁹ It has also been used, however, with less obvious validity to interpret phenomena which arise from the relatively short range interactions involved in the details of atom transfers,^{10,11} isotope effects,¹² and the occurrence of sticky collisions. The expression for the ion-induced dipole potential is derived in the perturbation and point dipole limits. Therefore, any accuracy it exhibits for intermolecular separation which are of the order of bond distances or for potential energies which

are appreciable fractions of typical electronic excitation energies, must be considered quite accidental. Moreover, the ion-induced dipole potential gives no information about the details of the bond making and breaking processes which are the essence of chemical reaction. It is clear that some more detailed guidance concerning the potential energy surface, even if of a qualitative nature, would be useful.

As any bimolecular reaction occurs, the molecular orbitals of the reactants interact and evolve into the orbitals of the collision complex and then into those of the product molecules. Consequently it is possible to make a correlation diagram which shows the connection between the orbitals of reactants and products. The simplest such diagrams are those which correlate atomic to diatomic molecular orbitals, and such diagrams have been a very great aid to the qualitative understanding of molecular stability. More recently, Herzberg¹³ has given several diagrams which correlate the molecular orbitals of polyatomic molecules with those of their atomic or molecular fragments. A few diagrams which correlated orbitals of the reactants and products of chemical reaction were given by Griffing,¹⁴⁻¹⁶ and it is her work which is the principal basis for the present paper. Another important early paper is by Schuler,¹⁷ who demonstrated how to use group theory to predict the possible electronic states of reaction products. Recently, Kaufman and Koski¹⁸ have extended and applied these methods to the O^+-N_2 reaction, and Gimarc¹⁹ has discussed the H_2-D_2 reaction in these terms. In addition, there has been a

a copious demonstration of the usefulness of correlation diagrams based on molecular orbital symmetry arguments in predicting the steric course of reactions and the geometry of molecules.

In what follows we shall construct and discuss molecular orbital correlation diagrams for several ion-molecule reaction. We confine ourselves here to reactions in which the hydrogen molecule is involved, since the most detailed dynamical information is available for these processes. The procedure to be followed is straightforward. A collision geometry, preferably with some symmetry elements, is selected, and the molecular orbitals of the reactants, intermediate complex, and, if possible, the products are resolved into species of the appropriate point group. Then, starting with those of lowest energy, reactant, intermediate, and product orbitals of the same species are connected. When no useful symmetry elements are present, the nodal structure of the orbitals serves as a guide. Mixing of orbitals of different symmetry under the influence of nontotally symmetric nuclear motions is considered. Considerable guidance concerning the order of orbital energies is available from ultraviolet and photoelectron spectroscopy, and SCF calculations. Some ambiguities can be resolved and predicted features of the potential energy surfaces can be verified by appearance potential information from mass spectrometry. The resulting diagrams are strictly qualitative, but do allow one to understand several apparently paradoxical experimental findings, and provide a more rational basis for

the discussion and prediction of reaction dynamical features than has been available in the past.

THREE ATOM SYSTEMS

First we consider the correlation diagram for a linear three atom system which would apply to the He-H_2^+ reaction. The appropriate form for the diagram has been given by Griffing and Vanderslice,¹⁵ and Fig. 1 is an adaptation of their diagram to the $(\text{He-H}_2)^+$ system. By using ionization energies to measure orbital energies, we see that for the reactants, the $1s$ orbital of helium lies lowest, with the energy of -24.6 eV. The σ_g orbital of H_2 is approximately 9 eV higher, and the σ_u^* orbital about 10 eV higher still. As He and H_2^+ approach, the He $1s$ orbital evolves into a nodeless σ bonding orbital of the HeHH^+ complex, and drops in energy. This orbital correlates to the nodeless 1σ bonding orbital²⁰ of HeH^+ . The σ_g orbital of H_2 is raised in energy as the reactants approach, and starts to correlate with the 2σ orbital of HeH^+ , which is strongly antibonding.²⁰ On the other hand, the σ_u^* orbital of H_2 initially drops in energy, and starts to correlate with the $1s$ orbital of the hydrogen atom. The impending crossings of the two uppermost zero-order orbitals is avoided, and their interaction produces two new orbitals. The lower of these has one node located approximately at the central H-atom, and is therefore weakly antibonding between the end atoms. The upper orbital has two nodes, one between the central atom and each end atom. Consequently, it is strongly antibonding.

If one enters the initial electron configuration for $\text{He} + \text{H}_2^+$ on the diagram, it is clear that these reactants evolve adiabatically and by a minimum energy path to $\text{HeH}^+(1\sigma)^2$ and $\text{H}(1s)^1$. This is consistent with the reaction



which has a substantial cross section for kinetic energies above the threshold.

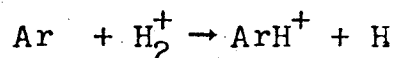
In contrast, the electron configuration which corresponds to $\text{He}^+ + \text{H}_2$ leads to a more complicated situation. Only one electron is initially in the orbital which correlates to the 1σ bonding orbital of HeH^+ . There are two possible fates for the two electrons that are initially in $\text{H}_2(\sigma_g)$. Both might end up in $\text{H}(1s)$, giving the very high energy products HeH^{++} and H^- . Alternatively, one electron might enter $\text{H}(1s)$, and the other the 2σ antibonding orbital of HeH^+ . The consequence of the latter disposition would be a normal hydrogen atom plus an excited, unbound $\text{HeH}^+(1\sigma)^1(2\sigma)^1$ which would separate to He^+ and H . The result of $\text{He}^+ - \text{H}_2$ collisions would be simply the dissociation of hydrogen, if sufficient initial relative kinetic energy were available, or the inelastic and elastic scattering of He^+ at lower energies.

The latter prediction seems consistent with experimental observations. The cross section²¹ for atom transfer to He^+ from H_2 is less than 10^{-18} cm^2 , and for dissociative charge exchange,²² less than 0.6 \AA^2 .

The $(\text{Ne-H}_2)^+$ system behaves essentially identically^{2,3,22} to the $(\text{He-H}_2)^+$ system. Formation of NeH^+ from Ne and H_2^+ is well known, but no chemical products from the charge exchanged reactants have been detected. The orbital correlation diagram for $(\text{Ne-H}_2)^+$ is very similar to Fig. 1, since the ionization energies of H_2 (15.5 eV) and Ne (21.4 eV) are quite different, and the first excited state of NeH^+ , like that of HeH^+ , is very probably unbound. Thus, as was predicted for He^+ , Ne^+ should be scattered elastically, inelastically, and at high energies, with dissociation of H_2 . In fact, we have found experimentally²³ that at high relative energies (16 eV) Ne^+ is back scattered from D_2 both elastically, and inelastically with a large relative energy loss (7 eV).

We see that correlation diagrams lead to an explanation of the apparently puzzling behavior of the $(\text{He-H}_2)^+$ and $(\text{Ne-H}_2)^+$ systems. This success or integrity of the correlations can in large measure be attributed to large difference in the ionization energies of hydrogen and the lighter rare gases, which leads to well-separated potential surfaces for the two initial charge states. Such dramatic chemical inequivalence of reactants and their charge exchanged state may well occur in other systems, for example, $\text{F}^+ + \text{Li}_2$ or $\text{Mg}^+ + \text{H}_2$. When the highest occupied orbitals of the reacting partners have nearly the same energy, however, we would expect that a pair of reactants and their charge exchanged state would produce the same chemical products.

An example of the latter situation occurs in the $(\text{Ar-H}_2)^+$ system. Both the reactions



are known to be rapid. A correlation diagram appropriate for them is shown in Fig. 2. The ionization energy of Ar to its ground $^3P_{3/2}$ state is 15.76 eV, and can be taken as the energy of the 3p orbital of Ar. The energy of the σ_g orbital of H_2 is rather ill-defined, however. While the adiabatic ionization energy of H_2 is 15.45 eV, the vertical ionization energy is 16 eV, and the vertical recombination energy of H_2^+ is 14.5 eV. Depending on which of these is chosen as the energy of the σ_g orbital, it is degenerate with, or lies below or above the 3p orbital of Ar. Consequently, we indicate the position of $\text{H}_2(\sigma_g)$ by a band of approximately 2 eV amplitude in Fig. 2.

The significance of this uncertainty in the orbital energy is considerable. In constructing and interpreting the correlation diagrams, we are following the zero order rule that the valence orbital of lowest energy in the reactants correlates with the lowest energy orbital of the product. If the reactant orbitals are degenerate or nearly so, this unique association cannot be made. Consequently, the systems Ar^+-H_2 and $\text{Ar}-\text{H}_2^+$ must be considered equivalent, and both correlate to the ground state orbital occupancy of the collision complex and the reaction products.

There is another way of looking at this problem. The most appropriate value for the energy of the σ_g orbital in H_2 might be the vertical ionization energy, 16 eV. Thus for the Ar^+-H_2 reaction, we might assume that it is the lower energy, doubly occupied $H_2(\sigma_g)$ orbital which correlates to the lowest orbital of ArH^+ . Since this orbital is doubly occupied, the products are formed in their ground states. For the $Ar-H_2^+$ reaction, the appropriate energy for the hydrogen σ_g orbital might be 14.5 eV, the vertical recombination energy for H_2^+ . Thus in this case the lowest reactant orbital is the doubly occupied $Ar(3p)$, which now correlates with the product ground state. Once again, adiabatic correlation forms products in their ground states, and we conclude that both charge states of $(Ar-H_2)^+$ are equivalent. The same argument applies to $(Kr-H_2)^+$, where similar behavior is observed experimentally.

The uncertainty in orbital energies becomes even more important for polyatomic ions and molecules. In interpreting the correlation diagrams for such systems, it must be remembered that sometimes rather small distortions in the nuclear framework can bring the energies of certain molecular orbitals into near coincidence, and thereby greatly influence the correlations between reactants and products.

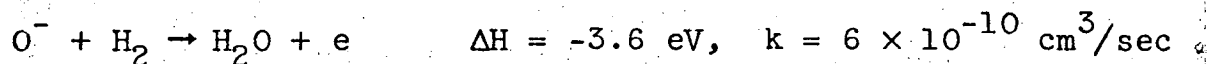
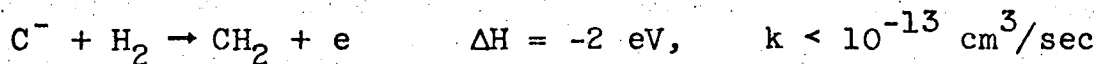
For the reactions of atomic ions like C^+ , N^+ , O^+ , and F^+ with H_2 , one may ask whether an insertion of the ion to form a bent or linear $H-X-H^+$ ion can occur. Were such ions formed from reactants in their ground states, the velocity vector distributions of the eventual reaction products HX^+ and H might

show the symmetry associated with the occurrence of a persistent collision complex for low collision energies. To treat this problem, we assume that the atomic ion approaches along the perpendicular bisector of the H_2 bond, and the C_{2v} symmetry is maintained until valence interactions have begun. We use the resulting correlation diagram between reactant orbitals and those of the bent and linear complexes to decide whether the ground state of the complex can be reached adiabatically, and also to consider whether orbital mixing which results from distortions from C_{2v} symmetry is important.

We begin by resolving the orbitals of the ion and H_2 into the species of C_{2v} . This can be done with the assistance of tables provided by Herzberg,¹³ or in this simple case, by inspection. The σ_g and σ_u orbitals of hydrogen transform as a_1 and b_2 in C_{2v} , while the p orbitals of the heavy atom resolve into a_1 , b_1 , and b_2 . The orbital energy level diagram for bent and linear H-X-H molecules has been given by Walsh,²⁵ and it is a simple matter to make the appropriate correlations which result in the diagram in Fig. 3. The H_2 σ_g orbital is set below the 2p atomic orbitals, but the modifications which must be made when these levels are reversed are obvious.

We must expect that there will be no crossing of the a_1 orbitals which originate as σ_g and $p\sigma$ of the reactants, and consequently an avoided crossing is shown. The question of whether deviation from C_{2v} symmetry mixes the a_1 and b_2 orbitals sufficiently to lead to an avoided crossing cannot be answered without detailed calculations for specific cases. For the present, we shall assume that no mixing occurs.

Now consider the two associative detachment reactions^{26,27}



Since the ground state of C^- is $4s$, we have one electron in the a_1 , b_1 , and b_2 p orbitals, all with parallel spins. Thus from Fig. 3 we see that the reactants evolve to the valence electron configuration $(2a_1)^2 (1b_2)^1 (3a_1)^2 (1b_1)^1 (4a_1)^1$. If we then imagine that the highest energy $4a_1$ antibonding electron is detached, we are left with a substantially excited state of CH_2 which has one $1b_2$ bonding electron promoted to the $3a_1$ nonbonding orbital. Thus the adiabatic autodetachment reaction would not be possible in thermal energy collisions. However, if there were mixing of the $3a_1$ and $1b_2$ orbitals, induced by departures from C_{2v} symmetry, the ground state configuration of CH_2 could be reached, and the detachment reaction would be energetically possible. Since the reaction has a rate constant²⁶ which indicates that detachment occurs less frequently than one in 10^4 collisions, it appears that the $3a_1$ and $1b_2$ orbitals do not mix appreciably.

For the O^- - H_2 reaction, in at least some of the collisions the O^- will have the p-electron configuration $(a_1)^1(b_1)^2(b_2)^2$. Figure 3 shows that this configuration, with detachment of the $4a_1$ electron, does evolve to the ground state of the H_2O molecule. The reaction does in fact occur with large, but less than unit collision frequency.²⁷ Thus the correlation diagram, interpreted in a straightforward manner, is consistent with

two experimental facts. We are unable, however, to explain on this basis why the S^-H_2 associative detachment reaction does not occur.²⁸

Application of the correlation diagram to the reactions of ground state C^+ , N^+ , O^+ , and F^+ with H_2 leads to the conclusion that in the absence of a_1-b_2 orbital interaction in no case can the ground electronic configuration of the intermediate HXH^+ molecular ion be reached adiabatically from the reactants. All four reactions can give XH^+ by a direct interaction through a linear XHH^+ complex, and consequently we expect to observe the asymmetry characteristic of direct interactions in the product velocity vector distributions. Only the N^+-H_2 reaction has been studied by measurement of product angular distributions,²⁹ and it has been found to proceed by a direct interaction mechanism at relative energies above 3.7 eV. However, before any firm conclusion concerning the accessibility of the ground state of NH_2^+ is reached, the reaction should be studied at lower relative energies. The $C^+(H_2,H)CH^+$ reaction has been studied with a fixed tandem mass spectrometer³⁰ but apart from the finding that there is no barrier in excess of the endothermicity, no explicit information on the dynamics of the reaction was obtained. Further investigations of this closely related series of reactions at low relative energies should be valuable.

FOUR CENTER SYSTEMS

Here we consider such reactions as



Reactions 1-3 have been studied extensively^{5,6,8,31-33} by product velocity vector distribution measurements over a wide range of initial energies, and details of such experiments for the acetylene-deuterium reaction will be reported subsequently.³⁴ There are some clear chemical similarities among these reactions, but the most important for our purposes is that in each case, the ground state potential energy surface has a substantial minimum for at least one configuration of the atoms. That is, the ions H_2CO^+ , N_2H_2^+ , H_2O_2^+ , and C_2H_4^+ are well known in mass spectrometry, and their appearance potentials show that they lie 2.5 to 3 eV below the separated reactants in reactions 1-4. Considering this common feature and the similar molecular complexities it has been quite surprising to find that reactions 1 and 2 proceed by direct interaction mechanisms even at quite low energies, while in reactions 3 and 4, persistent complexes are involved.

We consider reaction 1 as involving a collision which maintains C_{2v} symmetry until the intermediate H_2CO^+ is formed. The orbitals of CO^+ and H_2 are resolved into the species of

C_{2v} , and then systematically correlated with the orbitals of formaldehyde. The resulting correlation diagram is shown in Fig. 4. An approximate energy scale is provided, with the energies of the various orbitals of the reactants and intermediate located using the results of photoelectron and ultraviolet spectroscopy.^{13,35} The positions of the higher antibonding orbitals, the orbitals of HCO^+ , and of the crossing points are largely conjecture. While the energetics of the H_2-CO^+ system have guided construction of the diagram, no emphasis is placed on the numerical values of the energies, so the diagram should be applicable with minor modifications to any $H_2-X_2^+$ or H_2-XY^+ system in which the order of the orbitals is similar.

As H_2CO^+ is formed from H_2 and CO^+ , we expect the oxygen 2s orbital to remain essentially unchanged, while the carbon 2s and hydrogen σ_g orbitals combine to form a pair of orbitals which initially correlate with an $a_1-a_1^*$ pair which are C-H bonding and antibonding. The $p\sigma$ bonding orbital of CO^+ starts to correlate with the C-O σ bonding orbital of formaldehyde. As a result, there is an avoided crossing of two a_1 orbitals, and the σ_g orbital of H_2 appears to correlate with the C-O σ orbital of formaldehyde, while the σ orbital of CO^+ correlates with the C-H antibonding a_1^* orbital of formaldehyde. The other correlations are quite straightforward. One π orbital of CO^+ correlates with the π bonding orbital of H_2CO^+ , while the other combines with the σ_u^* orbital of hydrogen to produce

a C-H bonding-antibonding pair. The b_2^n nonbonding orbital of formaldehyde comes largely from the $b_2 \pi^*$ orbital of CO^+ .

Consider now the adiabatic evolution of $\text{CO}^+(^2\Sigma^+)$ and $\text{H}_2(^1\Sigma_g^+)$ into the complex H_2CO^+ . One electron is missing from the bonding σ orbital of CO^+ , so depending on the strength of the interaction between the highest occupied a_1 orbitals of the reactants, either one or two electrons will occupy the a_1^* C-H antibonding orbital of H_2CO^+ . No electrons are found in the b_2^n orbital. Thus the orbital occupation reached adiabatically in the collision is not that of the ground state of H_2CO^+ , but is that of an excited configuration which has one electron in a C-H antibonding orbital, and no electrons in the non-bonding b_2^n orbital. In terms of the species of C_{2v} , the reactants correlate to a 2A_1 state of the complex, whereas the ground state of the complex is 2B_2 . If this is an accurate description of the evolution of the system in a collision, then it is not surprising that the effects of the potential well associated with the ground state of H_2CO^+ are not evident in the angular distribution of products.

It may be argued that since the highest occupied a_1 orbital of the reactants crosses the empty b_2 orbital, the system can evolve to the ground state of H_2CO^+ if the a_1 and b_2 orbitals are coupled by the antisymmetric b_2 bending or stretching motion of the CH_2 group. This interaction might be expected to be weak, however, since the two orbitals concerned are largely concentrated on opposite ends of the H_2CO^+ molecule.

Therefore, the conclusion that H_2 and CO^+ correlate only with excited states of H_2CO^+ seems quite secure.

There is experimental evidence which supports this conclusion. The measured³⁶ appearance potential of CO^+ from H_2CO is 4.5 volts above the value calculated from the heats of formation of H_2 , CO^+ , and H_2CO . This shows that there is indeed a potential barrier between $H_2 + CO^+$ and H_2CO^+ which is 4.5 eV high. Since 4.5 eV is approximately the bond dissociation energy of H_2 , the value of the appearance potential of CO^+ from H_2CO suggests that two hydrogen atoms, rather than H_2 , may be formed along with CO^+ . Thus, either there is a 4.5 eV barrier between $H_2 + CO^+$ and ground state H_2CO^+ , or only $2H + CO^+$ can correlate with ground state H_2CO^+ . In either case, the potential well of H_2CO^+ is not accessible in low energy collisions of H_2 and CO^+ .

If we consider the evolution of ground state H_2CO^+ to $H + HCO^+$, we find from the correlation diagram no reason to expect a barrier in excess of the minimum energy necessary to form products. In confirmation of this, the appearance potential of HCO^+ from formaldehyde⁷ is in fairly good agreement with the value calculated from thermodynamic data (including the admittedly uncertain proton affinity of CO^+).

The following picture emerges from the correlation diagram and appearance potentials. As shown schematically in Fig. 5a, H_2 and CO^+ approaching in the C_{2v} configuration encounter a 4.5 eV barrier before reaching the region of minimum potential energy. Systems which have enough energy to surmount this barrier are very unstable with respect to $H + HCO^+$, and thus

spend only a very short time as H_2CO^+ . A calculation using RRKM unimolecular reaction rate theory and the energetics of Fig. 5a indicates a maximum lifetime for H_2CO^+ which is of the order of one or two vibrational periods. The products of such processes will have an intensity distribution which is characteristic of a direct interaction. When the reactants have less than 4.5 eV initial relative energy, the region of minimum potential energy cannot be reached, and no long-lived complexes are formed.

Since the reaction between CO^+ and H_2 has a large cross section even for relative energies below 0.1 eV, there must be a path between reactants and products which does not have a potential energy barrier. This leads us to construct the correlation diagram for collinear $\text{H}_2\text{-CO}^+$ configurations shown in Fig. 6. There is very little guidance from experiment available to aid the construction of this diagram, aside from the orbital energies of the reactants and those of HCN, which is isoelectronic to HCO^+ . It is clear, however, that the π orbitals of CO evolve in a straightforward way into those of HCO^+ . The σ orbitals may be correlated by recognizing that to a first approximation the σ_g and σ_u^* orbitals of H_2 and the 2s orbital of carbon combine in the same manner as is shown in Fig. 1 for the $\text{H}_2\text{-He}$ system. This simple scheme, which would result in $2s(\text{C})$, $\sigma_g(\text{H}_2)$ and $\sigma_u^*(\text{H}_2)$ correlating respectively with $\sigma(\text{C-H})$, $1s(\text{H})$, and $\sigma^*(\text{C-H})$ of the HCO^* and H products, is complicated by the crossings of these σ orbitals with the

bonding and antibonding σ orbitals of the CO group. These interactions lead to the avoided crossings indicated in Fig. 6.

We now introduce the 11 valence electrons of the $H_2 + CO^+$ system. The σ orbital of CO^+ is occupied by only one electron, with all lower orbitals filled. It is clear that as the system evolves toward $H + HCO^+$, the ground state electron configuration is maintained, and thus there is no reason to expect any substantial potential energy barriers to occur. At qualitative assessment of the bonding character of the occupied orbitals does not suggest the occurrence of any particularly deep potential well for any linear configuration. Thus the potential seems to have the qualitative characteristics which are required to explain reaction by direct interaction at even the lowest relative energies of collision.

To summarize: A correlation diagram suggests, and appearance potential measurements confirm, that there is a 4.5 eV barrier between $H_2 + CO^+$ and the ground state of C_{2v} H_2CO^+ . Thus the potential well corresponding to H_2CO^+ is not accessible in low energy collisions of H_2 and CO^+ . The correlation diagram for collinear collisions suggests that there are no high barriers or deep wells between reactants and products for these configurations. The reaction should therefore proceed by a direct interaction mechanism at all energies, as is observed experimentally.

We turn now to the $N_2^+ - H_2$ system. Here the stable intermediate which might give rise to a persistent collision complex is the di-imide ion, $HN=NH^+$. We must therefore construct a

correlation diagram for the approach of N_2^+ to H_2 which leads to one hydrogen atom on each nitrogen and which maintains C_{2v} symmetry.

The result is shown in Fig. 7. The essentially nonbonding $2s$ a_1 and b_2 orbitals of N_2 in combination with the σ_g and σ_u^* orbitals of H_2 produce $a_1-a_1^*$ and $b_2-b_2^*$ N-H bonding and antibonding orbital pairs in $N_2H_2^+$. The σ_g-a_1 and $\sigma_u^*-b_2^*$ bonding and antibonding orbitals of N_2 evolve into the corresponding orbitals of $N_2H_2^+$. One $\pi-\pi^*$ (out of plane) orbital pair of nitrogen is essentially unchanged, while the other, in-plane, $\pi-\pi^*$ pair of orbitals becomes the a_1^n and b_2^n nonbonding orbitals of $N_2H_2^+$. The correlations to the orbitals of a linear HAAH molecule are also given in Fig. 7, so that the diagram can be used to discuss formation of $C_2H_2^+$ from C_2^+ and H_2 , for example.

Insertion of the 11 valence electrons of N_2^+ and H_2 into the lowest reactant orbitals leads to the conclusion that $N_2H_2^+$ would be formed adiabatically with at least one electron in the a_1^* N-H antibonding orbital. This conclusion would be consistent with the fact that ion beam experiments have produced no evidence that a persistent complex occurs in this reaction. However, if one considers the possibility of orbital mixing by electronic-vibrational interaction, the situation becomes somewhat ambiguous. Distortions of species B_2 may eliminate the crossings of the curves leading to the a_1^* and b_2^n orbitals of $N_2H_2^+$, and thereby allow adiabatic evolution of the reactants to the ground state of $N_2H_2^+$. This vibronic interaction and

mixing of the a_1^* and b_2^n orbitals could very easily be strong, since in contrast to the situation in the H_2CO^+ case, the orbitals overlap rather substantially. However, even with the occurrence of this vibronic mixing, some potential barrier between the reactants and $N_2H_2^+$ might remain, and prevent low energy reactants from reaching the regions of potential energy minima.

Unfortunately, there has been no published measurement of the appearance potential of N_2^+ from N_2H_2 , so it is not possible to use experimental data to resolve the question of the existence or importance of this barrier, as was done for the CO^+-H_2 system. However, an answer to this question is not necessary in order to decide why no persistent complex is observed in the $N_2^+-H_2$ system. Figure 5b shows the relative enthalpies of, $N_2^+ + H_2$, $N_2H_2^+$, and $N_2H^+ + H$ which can be calculated from tabulated data and the proton affinity of N_2 recently measured by Schiff and coworkers.³⁷ The potential well of $N_2H_2^+$ is only approximately 0.5 eV deep with respect to $N_2H^+ + H$, and no dissociation barrier in excess of this is expected. If we assume that there is no barrier between $N_2^+ + H_2$ and $N_2H_2^+$, then even complexes formed by essentially zero energy collisions between N_2^+ and H_2 would have a total energy six times the minimum necessary to decompose to products. Consequently, the lifetime of such complexes would be very small, approximately 2×10^{-14} sec, according to an RRKM calculation. This is so short that the reaction will appear to proceed by direct interaction. If

any barrier between reactants and the complex does exist, reactants with enough energy to cross it will form "complexes" whose lifetimes would be even shorter than 2×10^{-14} sec. Moreover, the direct interaction path through linear HHNN^+ is also available to the system, and will undoubtedly contribute to the scattering pattern.

To summarize, we can say that it is likely that vibronic coupling makes the N_2H_2^+ potential well accessible to N_2^+-H_2 at some fairly small collision energy. However, even if this well is accessible at the lowest energies, the lifetime of the collision complex is expected to be much shorter than a rotational period, and the reaction will appear to go by a direct interaction mechanism. This is observed experimentally.

The correlation diagram which applies to the O_2^+-H_2 system is in many respects similar to that for the N_2^+-H_2 system. Once again we assume that C_{2v} symmetry is maintained as a nonlinear, planar, HOOH^+ molecule is formed from reactants. However, the σ bonding orbital in O_2^+ lies below, rather than above, the π_u orbitals, and the $2s$ orbitals of O_2 are lower than those in N_2 , and participate correspondingly less in the bonding. These considerations make no substantial change in the qualitative arguments which follow, and so Fig. 7 can be applied to the $(\text{O}_2-\text{H}_2)^+$ system.

In the $\text{O}_2^+(^2\pi_g)-\text{H}_2$ system, one electron occupies the π_g^* orbital of O_2^+ , and all lower orbitals are filled. An adiabatic evolution to H_2O_2^+ would produce a highly excited molecule with the configuration $(1a_1)^2 (1b_2)^2 (2a_1)^2 (2b_2)^1 (3a_1)^2 (1b_1)^2 (1a_2)^0 (4a_1^*)^2$. However, the crossing of the orbitals which

correlate to $\sigma_g(\text{H}_2)$ and $\pi_g^*(\text{O}_2)$ may be eliminated by vibronic interaction produced by the B_2 bending and stretching modes of H_2O_2^+ . In addition, coupling between the antibonding $4a_1^*$ orbital and the a_2 orbital might arise from the torsional motion of A_2 species, but the strength of this coupling might be small. Consequently, the initial correlation of the $\sigma_g(\text{H}_2)$ orbital to the $4a_1^*$ antibonding orbital, even if modified by vibronic mixing, would seem to produce a potential energy barrier between $\text{H}_2 + \text{O}_2^+$ and H_2O_2^+ . This supposition is confirmed by experiment,³⁸ since the appearance potential of O_2^+ from H_2O_2 indicates that there is a 2.5 ± 0.5 eV barrier between $\text{H}_2 + \text{O}_2^+$ and the potential well region of H_2O_2^+ .

Dissociation of a strictly planar H_2O_2^+ to $\text{H} + \text{HO}_2^+$ would produce an excited configuration of HO_2^+ with one electron excited from a σ^n nonbonding orbital to the π^* orbital. This correlation to excited products can be avoided if H_2O_2^+ is nonplanar, since this situation permits interaction and mixing of the π^* and σ^n orbitals. This may very well be the correct description of H_2O_2^+ since the appearance potential of HO_2^+ from H_2O_2 shows that the ground state is formed, and that there is no barrier between H_2O_2^+ and $\text{H} + \text{HO}_2^+$ in excess of the dissociation energy.

We are led, therefore, to the potential energy profile given in Fig. 5c. The reason why a long-lived H_2O_2^+ collision complex occurs^{39,40} even for initial relative energies as high as 5 eV is now clear. There is a deep potential well which is

a consequence not only of the stability of H_2O_2^+ , but of the potential barrier in the reactant channel. Thus in this case the tendency for the reactants to correlate in the lowest approximation to an excited state of the complex actually produces the feature which is in large measure responsible for the occurrence of a persistent complex.

We can also use Fig. 7 to analyze the reaction of metastable $\text{O}_2^+(^4\pi_g)$ with hydrogen. In $\text{O}_2^+(^4\pi_g)$, only one electron occupies the σ bonding orbital, while the two π_g^* orbitals each have one electron. The correlation diagram shows that this necessarily leads to an excited state of H_2O_2^+ , with one O-O σ -bonding electron excited to a $5 a_1^*$ O-H antibonding orbital. A long-lived complex would not be expected, and indeed experiment⁴¹ shows that the reaction proceeds by a direct interaction mechanism.

It is also useful to construct the correlation diagram for $\text{H}_2\text{-O}_2^+$ collisions under the assumption that the collision occurs through a planar nonlinear or L-shaped intermediate. In this case, one of the π_u orbitals of O_2^+ evolves to an O-H bonding orbital on one oxygen atom, while the corresponding π_g orbital becomes a nonbonding orbital on the other oxygen atom. The π_u and π_g^* orbitals perpendicular to the plane of the complex remain largely unchanged, as is also true in a first approximation for the σ_g and σ_u^* orbitals of O_2^+ . The σ_g and σ_u^* orbitals of H_2 evolve in the first approximation to an O-H antibonding orbital of HO_2^+ and the $1s$ orbital of the free

hydrogen atom. The resulting diagram, Fig. 8, has several curve crossings. Since the only useful symmetry operation of such a nonlinear planar complex is reflection in the plane of the molecule, it can be argued that there is strong mixing of all orbitals which are symmetric under this operation, and consequently all crossings of such orbitals are avoided.

Figure 8 has been drawn with this point in mind.

Several conclusions are possible from Fig. 8. First, $O_2^+(^2\pi_g)$ can react directly with H_2 via this nonlinear complex to give HO_2^+ and H . It has been suggested that the failure of the RRKM or quasiequilibrium theory to explain the relative intensities of the reaction products HO_2^+ , OH^+ , and H_2O^+ can be rationalized if some of the HO_2^+ is formed by a direct interaction process.⁴⁰ Second, the direct reaction between $O_2^+(^4\pi_g)$ and H_2 can occur through a nonlinear complex, but the product appears to be an excited configuration of HO_2^+ with one electron present in the π^* orbital, and one electron missing from the σ O-O bonding orbital. Similarly, the $H_2^+-O_2$ reaction would produce a configuration in which an electron had been excited from the σ^n orbital to the π^* orbital. Since the reaction of $O_2^+(^4\pi_g)$ with H_2 to form ground state HO_2^+ is 2.2 eV exothermic, it is possible that a low lying electronic state of HO_2^+ might be formed. The $H_2^+-O_2$ reaction is only 0.6 eV exothermic, however, so it is unlikely that an excited state of HO_2^+ could be produced by the reaction at room temperature. It seems likely that either the π^* orbitals are mixed by deviations

from planar geometry in the nonlinear O-O-H-H complex so that the system can evolve to ground state products, or the H_2^+-O_2 reaction proceeds through the complex which has the hydrogen peroxide structure, and which can dissociate to ground state products.

We consider now Fig. 9, the correlation diagram for the reaction of acetylene ion with hydrogen. The reactants approach with C_{2v} symmetry and evolve to the D_{2h} symmetry of ethylene. We assign the symmetry species of the orbitals consistently under the convention that the z-axis lies in the plane and is the perpendicular bisector of the carbon-carbon bond. The more conventional symmetry designations for ethylene which assume a z-axis perpendicular to the molecular plane are given in brackets.

The σ and σ^* orbitals of acetylene all evolve in a straightforward and obvious way to those of ethylene. The σ_g orbital of hydrogen combines with the in-plane π_u orbital of acetylene to produce a b_{2u} C-H bonding-antibonding pair of orbitals in ethylene, while $\sigma_u^*(\text{H}_2)$ and one $\pi_g^*(\text{C}_2\text{H}_2)$ give in a similar manner b_{3g} C-H bonding and antibonding orbitals of ethylene. Only one crossing of importance occurs, which is between the lines leading to the b_{3g} C-H bonding and b_{1u} C-H antibonding orbitals of ethylene. These two orbitals could be mixed by the two B_{2u} vibrations of ethylene, or by motions of species B_2 as the reactants approach with C_{2v} symmetry. Because the two orbitals overlap rather well and are probably both sensitive

to hydrogen motion, the vibronic coupling between them is probably large.

The acetylene ion has the configuration $\dots\pi_u^3$, and consequently, as $C_2H_2^+$ and H_2 collide with C_{2v} symmetry, one electron is present in the $\pi_u-a_1-b_{2u}$ orbital which is initially C-H antibonding. Because only one electron is in this orbital, and because of the vibronic coupling of b_{2u} to the C-H bonding $\pi^*-b_2-b_{3g}$ orbital, we do not expect a large activation barrier between the reactants and $C_2H_4^+$. This expectation is confirmed by the experimental observation⁷ that the appearance potential of $C_2H_2^+ + H_2$ from C_2H_4 is the same as that calculated from the relevant heats of formation. Since no potential barrier in excess of the bond energy is expected for the withdrawal of one hydrogen atom from $C_2H_4^+$, we expect the potential energy profile shown in Fig. 5d.

Inasmuch as the deep well corresponding to $C_2H_4^+$ is completely accessible in low energy collisions, we expect that the reaction between $C_2H_2^+$ and H_2 would show evidence of the occurrence of a persistent collision complex. We³⁴ have measured the velocity spectra at zero laboratory scattering and of $C_2D_2H^+$ from $C_2D_2^+ - H_2$ collisions. At high relative energies (5.5 eV) $C_2D_2H^+$ has its maximum intensity near the value calculated for spectator stripping, but as the initial relative energy is lowered, this peak moves toward the center of mass. At less than 3 eV initial relative energy, the distribution is symmetric about the center of mass velocity. While this is not an entirely

conclusive proof of the occurrence of a persistent complex, it is highly suggestive that the expectations derived from the correlation diagram are correct.

As a final example, we discuss the $\text{OH}^+(\text{H}_2, \text{H})\text{H}_2\text{O}^+$ reaction. Because of the great stability of H_3O^+ , it would seem likely that a persistent complex might occur in this reaction. The correlation diagram is most easily constructed if it is assumed that $\text{OH}^+(^3\pi)$ and H_2 approach in a T-shaped configuration of C_{2v} symmetry. The correlations are then very much like those in the $\text{H}_2\text{-CO}^+$ reaction. The resulting planar D_{3h} H_3O^+ is then allowed to relax to its equilibrium C_{3v} symmetry. There is, of course, no implication that the molecules rigidly follow this sequence of geometries in the reaction, but the introduction of the planar intermediate makes the correlation diagram easier to construct and also applicable to the $\text{CH}^+\text{-H}_2$ reaction. The result is shown in Fig. 10.

In $\text{OH}^+(^3\pi)$ two electrons with parallel spin occupy the two degenerate $p\pi$ orbitals, and all orbitals of lower energy are filled. As the reactants approach, vibronic interaction may mix the $\sigma_g a_1$ orbital of H_2 with the $p\pi b_2$ orbital of OH , but our analysis of the reactions of atomic ions with hydrogen seemed to be most consistent with the idea that this interaction was not important. The out of plane or umbrella motion of H_3O^+ would also tend to mix the $\sigma_g a_1$ and $p\pi b_1$ orbitals as H_2 approaches OH^+ . However, even if either or both of these interactions occurs, one electron will be found in the a_1^* O-H

antibonding orbital of H_3O^+ , if the electron spin conservation rule is obeyed. Therefore, the ground state of the H_3O^+ complex is not accessible to the reactants $\text{OH}^+(^3\pi)$ and $\text{H}_2(^1\Sigma)$, and no evidence for a persistent complex is expected. We³⁴ have measured the velocity spectra of H_2O^+ from this reaction at relative energies from 5.0 to 7.6 eV and find evidence for only a direct interaction process.

CONCLUSION

We have explored the application of molecular orbital correlation diagrams to a number of ion-molecule collision processes. In situations where the reactant and product orbitals are few in number and well spaced in energy, the correlation between reactant and product electronic configurations is clear and leads to several predictions which are consistent with known experimental facts. When the orbital energies are more closely spaced so that orbital energy degeneracies occur as reactants evolve to products, the correlation diagrams can be ambiguous. However, reference to measured ion appearance potentials can sometimes remove such ambiguities and provide a qualitative picture of the potential energy surface which is sufficient to predict the major features of the dynamics of a reaction. It would appear that despite their qualitative nature, as these diagrams are modified and refined in the light of new experimental and calculational data, they will provide an increasingly useful guide to the understanding of a variety of reactive collision processes.

Acknowledgements.- This work was supported by the U. S. Atomic Energy Commission. I would like to thank Dr. F. S. Mortimer for his suggestion that orbital correlations might be usefully applied to ion-molecule reactions.

References

1. H. von Koch and L. Freedman, J. Chem. Phys. 38, 1115 (1963).
2. W. A. Chupka and M. E. Russell, J. Chem. Phys. 49, 5426 (1968).
3. T. F. Moran and L. Friedman, J. Chem. Phys. 39, 2491 (1963).
4. V. Aquilanti, A. Galli, A. Giardini-Guidoni, and G. G. Volpi, J. Chem. Phys. 43, 1969 (1965).
5. A. Ding, A. Henglein, D. Hyatt, and K. Lacmann, Zeit. fur Naturforsch. 23A, 2084 (1968).
6. J. Kerstetter and R. Wolfgang, J. Chem. Phys. 53, 3765 (1970).
7. J. L. Franklin et al., Ionization Potentials, Appearance Potentials, and Heats of Formation of Gaseous Positive Ions, NSRDS-NBS 26 (1969).
8. E. A. Gislason, B. H. Mahan, C. W. Tsao, and A. S. Werner, J. Chem. Phys. 50, 5418 (1969).
9. E. W. McDaniel, V. Cermak, A. Dalgarno, E. E. Ferguson, and L. Friedman, Ion Molecule Reactions (Wiley-Interscience, New York, 1970).
10. D. T. Chang and J. C. Light, J. Chem. Phys. 52, 5687 (1970).
11. P. M. Hierl, Z. Herman, and R. Wolfgang, J. Chem. Phys. 53, 660 (1970).
12. T. F. Moran and L. Friedman, J. Chem. Phys. 42, 2391 (1965).
13. G. Herzberg, Electronic Spectra and Electronic Structure of Polyatomic Molecules (Van Nostrand, Princeton, New Jersey, 1966).

References (Continued)

14. V. Griffing, J. Chem. Phys. 23, 1015 (1955).
15. V. Griffing and J. T. Vanderslice, J. Chem. Phys. 23, 1039 (1955).
16. V. Griffing and J. S. Dooling, J. Phys. Chem. 61, 11 (1957).
17. K. E. Shuler, J. Chem. Phys. 21, 624 (1953).
18. J. J. Kaufman and W. S. Koski, J. Chem. Phys. 50, 1942 (1969).
19. B. M. Gimarc, J. Chem. Phys. 55, 1623 (1970).
20. H. H. Michels, J. Chem. Phys. 44, 3834 (1966).
21. C. F. Giese and W. B. Maier II, J. Chem. Phys. 35, 1913 (1961).
22. L. Friedman and T. F. Moran, J. Chem. Phys. 42, 2624 (1965).
23. B. H. Mahan and J. S. Winn, unpublished results.
24. C. F. Giese and W. B. Maier, J. Chem. Phys. 39, 739 (1963).
25. A. D. Walsh, J. Chem. Soc. (London) 2260 (1953).
26. F. C. Fehsenfeld and E. E. Ferguson, J. Chem. Phys. 53, 2614 (1970).
27. J. L. Moruzzi, J. W. Ekin, and A. V. Phelps, J. Chem. Phys. 48, 3070 (1968).
28. F. C. Fehsenfeld and E. E. Ferguson, J. Chem. Phys. 51, 3512 (1969).
29. E. A. Gislason, B. H. Mahan, C. W. Tsao, and A. S. Werner, J. Chem. Phys. 54, 000 (1971).
30. W. B. Maier, J. Chem. Phys. 46, 4991 (1967).

References (Continued)

31. W. R. Gentry, E. A. Gislason, Y. T. Lee, B. H. Mahan, and C. W. Tsao, *Discussions Faraday Soc.* 44, 137 (1967).
32. Z. Herman, J. Kestetter, T. Rose, and R. Wolfgang, *Discussions Faraday Soc.* 44, 123 (1967).
33. W. R. Gentry, E. A. Gislason, B. H. Mahan, and C. W. Tsao, *J. Chem. Phys.* 49, 3058 (1968).
34. B. H. Mahan, M. H. Cheng, and M. H. Chiang, unpublished results.
35. D. W. Turner, C. Baker, A. D. Baker, and C. R. Brundle, *Molecular Photoelectron Spectroscopy* (Wiley-Interscience, New York, 1970).
36. J. C. D. Brand and R. I. Reed, *J. Chem. Soc. (London)* 2386 (1957).
37. H. I. Schiff, 159th Meeting, Amer. Chem. Soc., Toronto, Canada, May 1970.
38. S. N. Foner and R. L. Hudson, *J. Chem. Phys.* 36, 2676 (1962).
39. E. A. Gislason, B. H. Mahan, C. W. Tsao, and A. S. Werner, *J. Chem. Phys.* 50, 5418 (1969).
40. M. H. Chiang, E. A. Gislason, B. H. Mahan, C. W. Tsao, and A. S. Werner, *J. Phys. Chem.* (to be published).
41. A. Ding and A. Henglein, *Ber. Bunsenges. Phys. Chem.* 73, 562 (1969).

Figure Captions :

- Fig. 1. A correlation diagram for the lowest orbitals of the linear $(\text{HeHH})^+$ system. The orbital energies are only semiquantitative, except for the atomic species. The lowest-order correlations are indicated by the dashed lines which cross.
- Fig. 2. A correlation diagram for the lowest orbitals of the linear $(\text{ArHH})^+$ system. The energy of the σ_g orbital of H_2 is indicated by a shaded band to represent the spread between the vertical ionization energy of H_2 and the vertical recombination energy of H_2^+ .
- Fig. 3. A correlation diagram for collisions of a heavy atom or ion x with H_2 . During their approach, the reactants are assumed to maintain C_{2v} symmetry. The crossing of the a_1^* and a_1^n curves in all probability is avoided.
- Fig. 4. A correlation diagram for CO^+-H_2 collisions. It is assumed that C_{2v} symmetry is maintained as the reactants approach. The circled crossings between the a_1 orbitals originating as $\sigma_g(\text{H}_2)$ and $\sigma(\text{CO})$ and $\sigma^*(\text{CO})$ probably are avoided.
- Fig. 5. Schematic representations of the principal features of four potential energy surfaces. (a) Surface for the $\text{CO}^+(\text{H}_2, \text{H})\text{HCO}^+$ reaction. The 4.5 eV barrier between reactants and products is established by the appearance potential of CO^+ from H_2CO^+ . (b) Surface for the $\text{N}_2^+(\text{H}_2, \text{H})\text{N}_2\text{H}^+$ reaction. The barrier suggested by the

Figure Captions (Continued)

correlation diagrams but unknown experimentally is indicated by the shaded area. (c) Surface for the $O_2^+(H_2, H)HO_2^+$ reaction. The location of the barrier and well are determined from appearance potentials. (d) Surface for the $C_2H_2^+(H_2, H)C_2H_3^+$ reaction. The barrier suggested by the lowest order orbital correlation but apparently eliminated by vibronic interaction is indicated by the shaded area.

- Fig. 6. A correlation diagram for the collinear reaction of CO^+ with H_2 . The circled crossings are probably avoided.
- Fig. 7. A correlation diagram for the addition of H_2 to a π system of a diatomic molecule to form either a bent or linear intermediate and eventually a linear triatomic product. The circled crossings are very probably avoided. It is assumed that the σ_g orbital of A_2 lies above the π orbitals, as would be the case for N_2 , but reversal of the order of these orbitals makes no important changes in the correlations.
- Fig. 8. A correlation diagram for the reaction $O_2^+(H_2, H)HO_2^+$ proceeding through a nonlinear collision complex.
- Fig. 9. A correlation diagram for the addition of H_2 to C_2H_2 . The molecular orbitals are labeled assuming that the z-axis is the perpendicular bisector of the carbon-carbon bond. The designations for the ethylene orbitals

Figure Captions (Continued)

assuming that the z axis is perpendicular to the molecular plane are given in brackets.

Fig. 10. A correlation diagram for the $\text{OH}^+(\text{H}_2, \text{H})\text{H}_2\text{O}^+$ reaction and other similar reactions in which the intermediate may be planar or pyramidal.

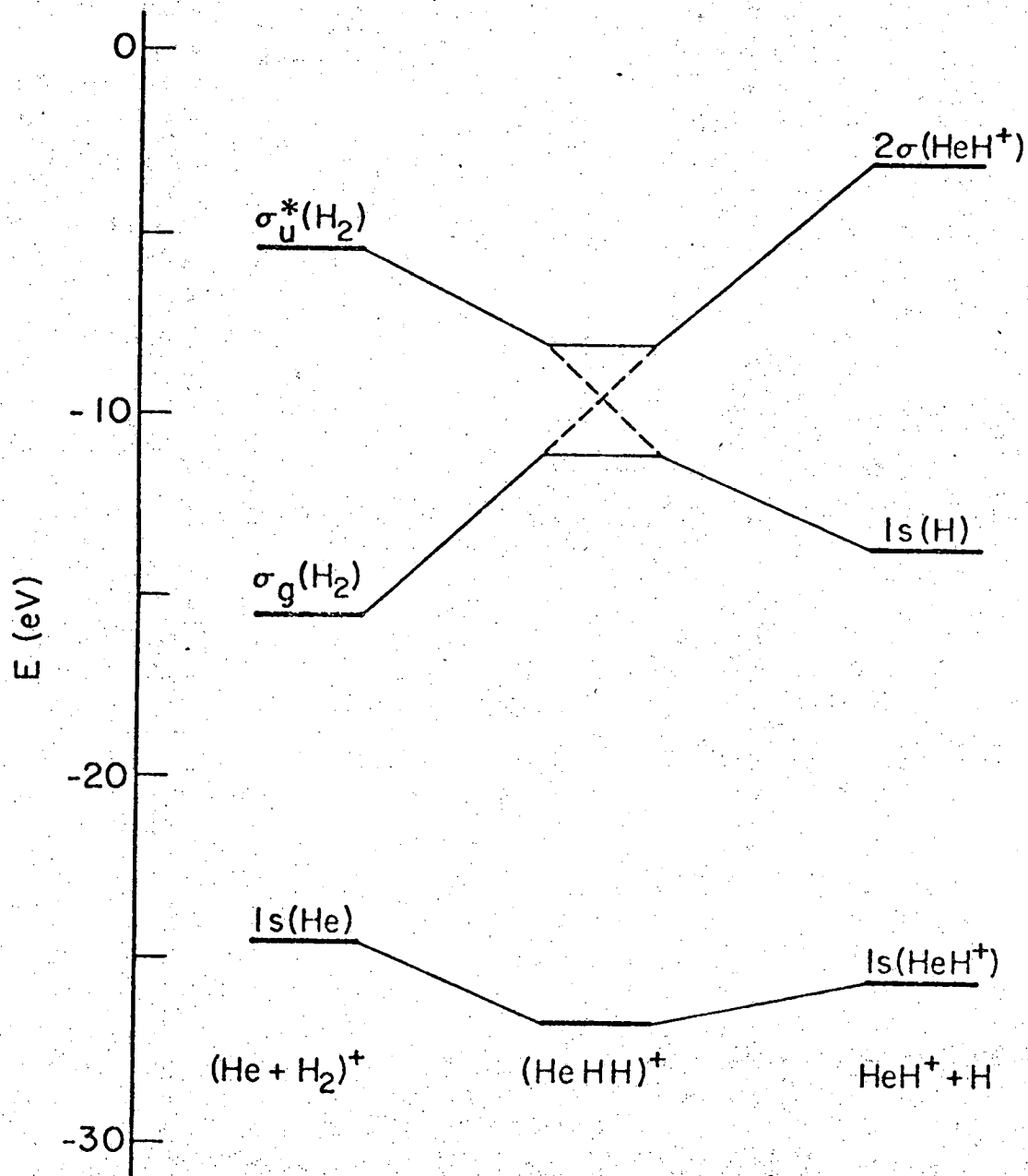


Fig. 1

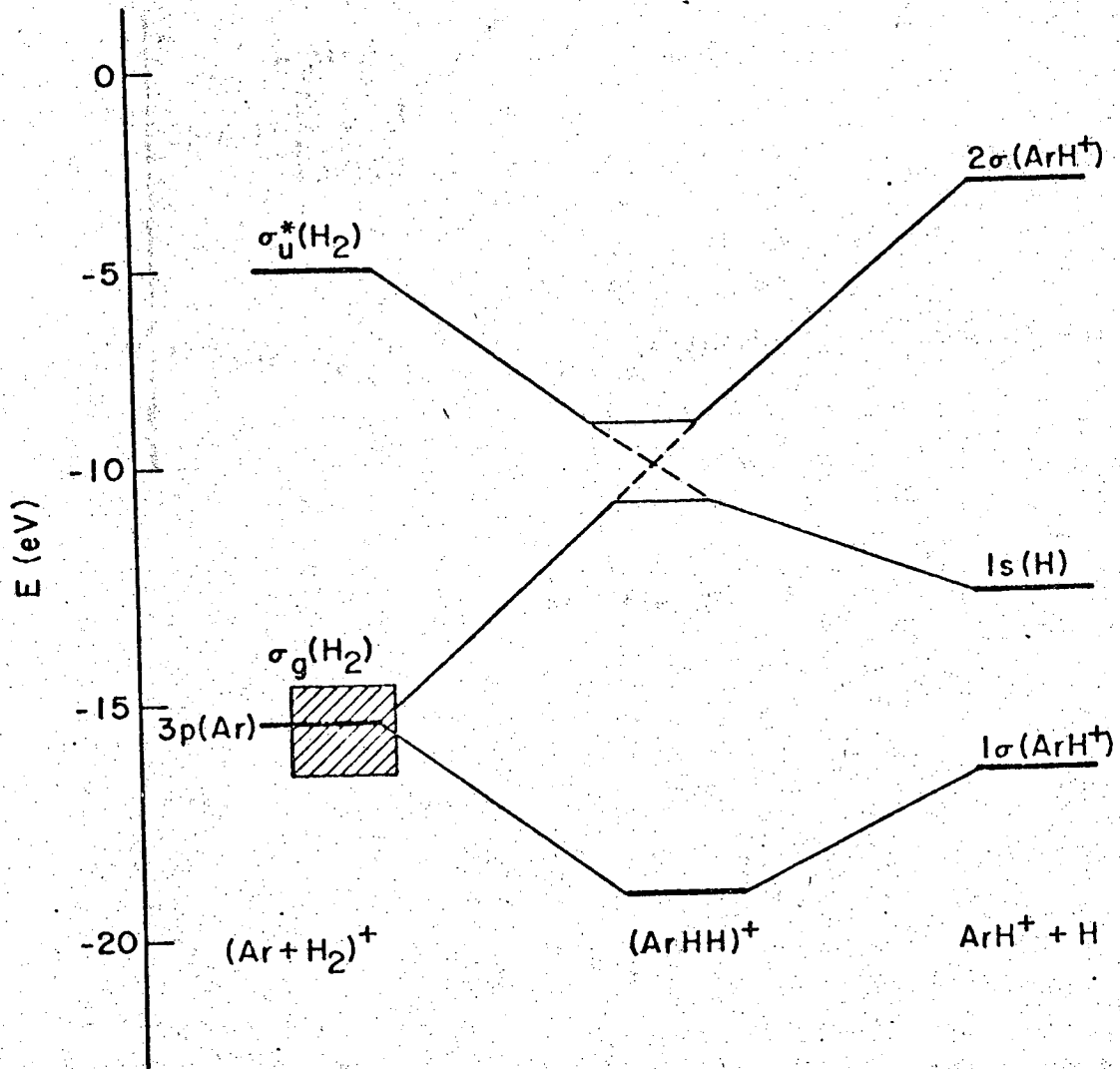


Fig. 2

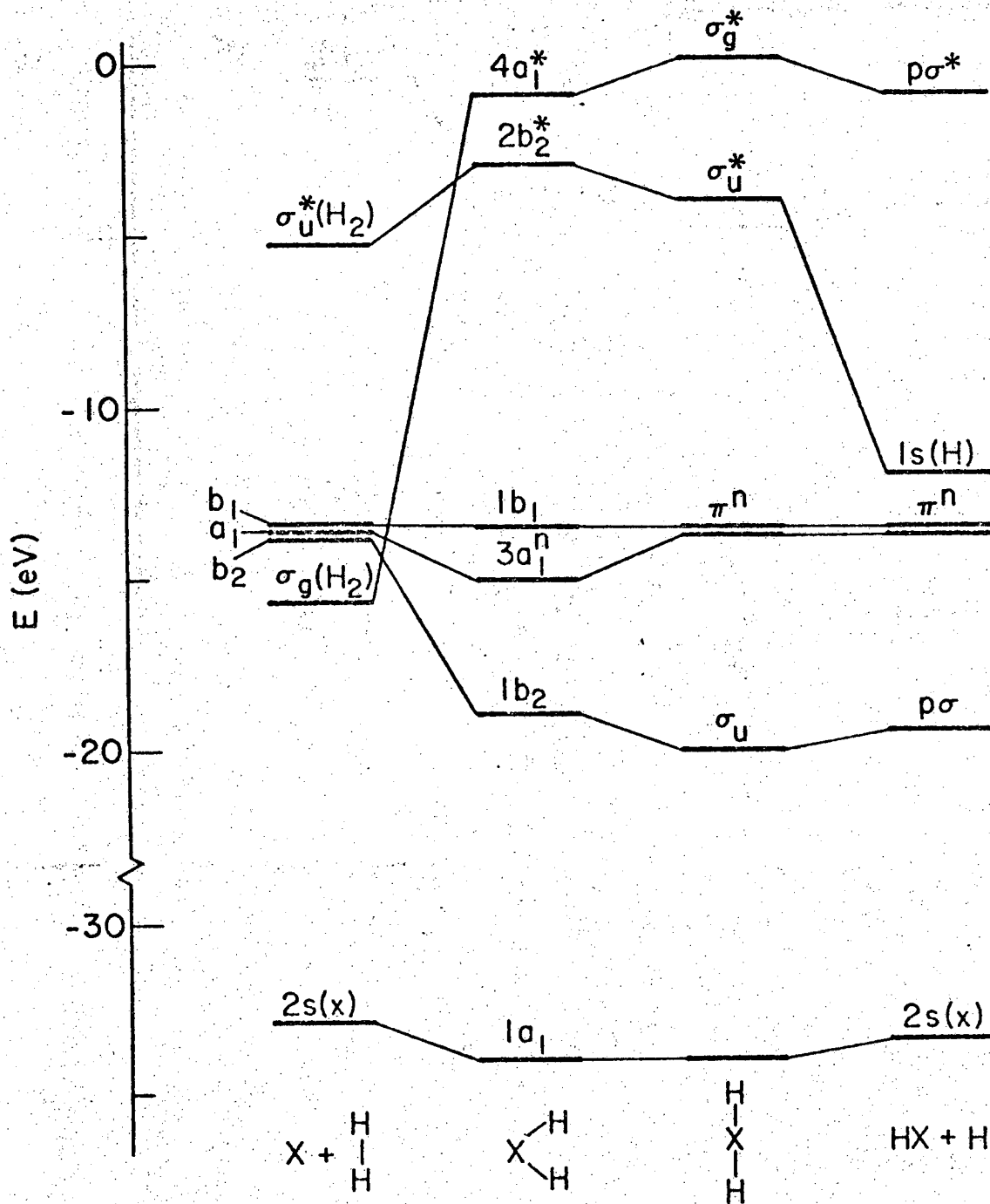


Fig. 3

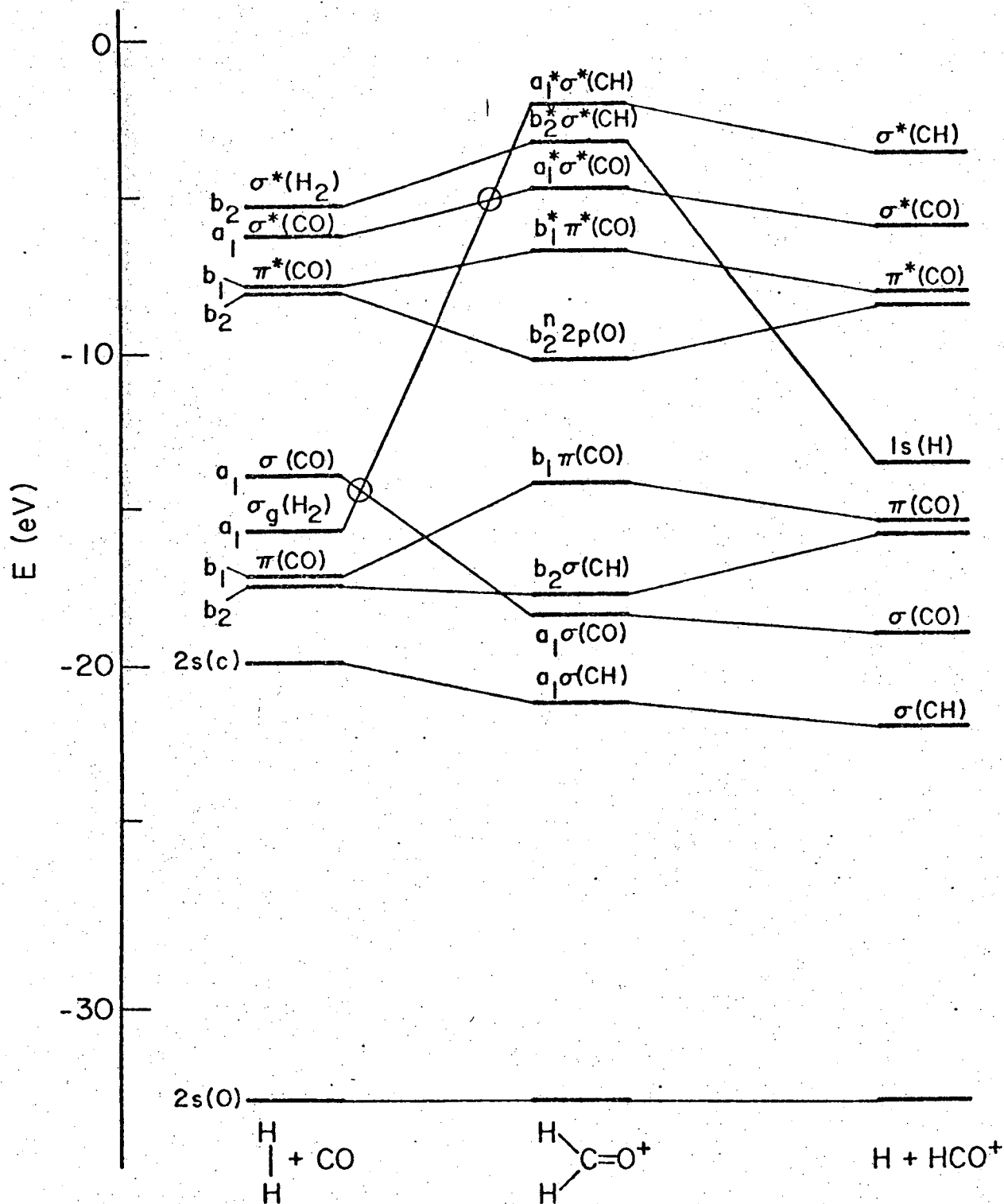


Fig. 4

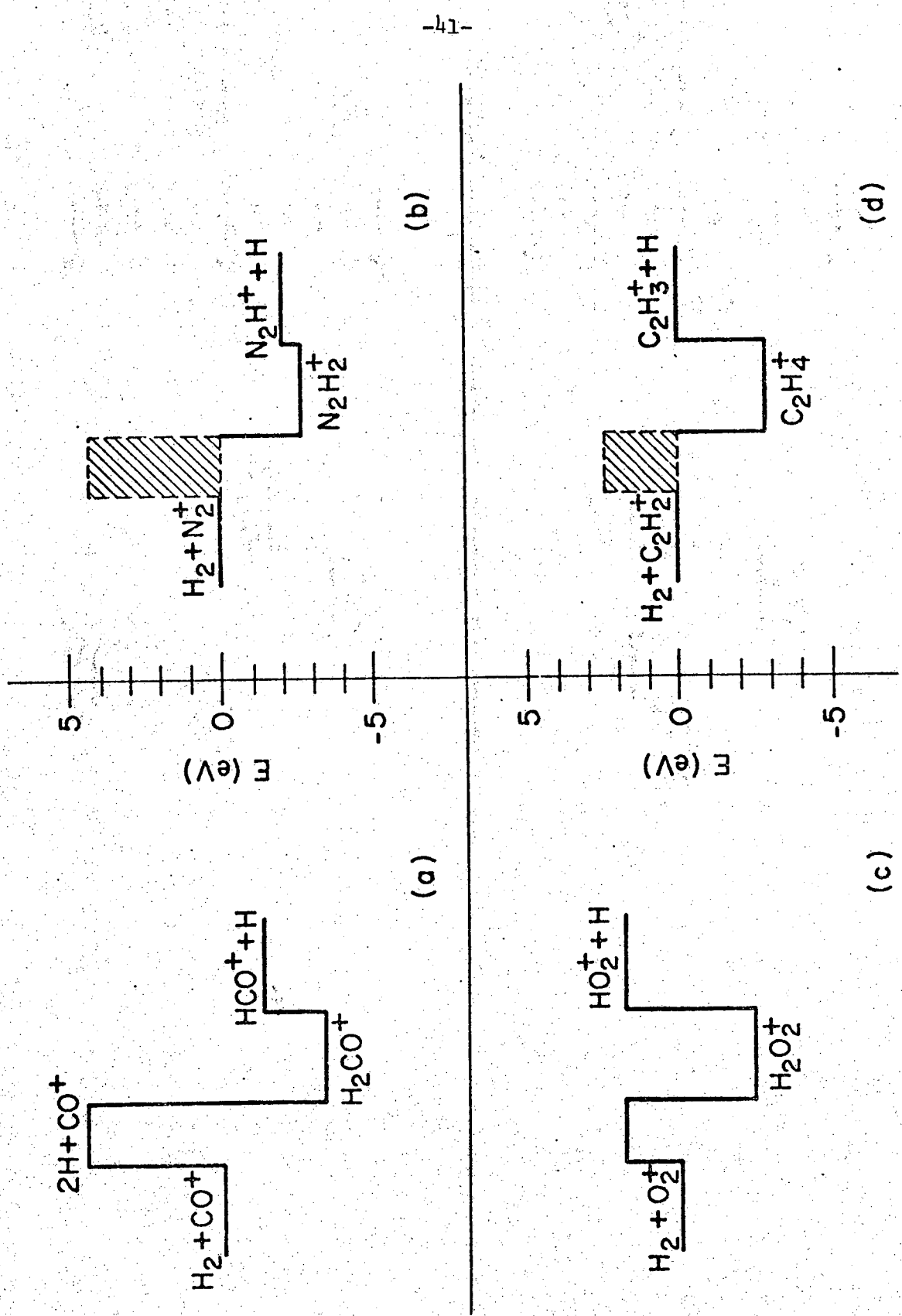


Fig. 5

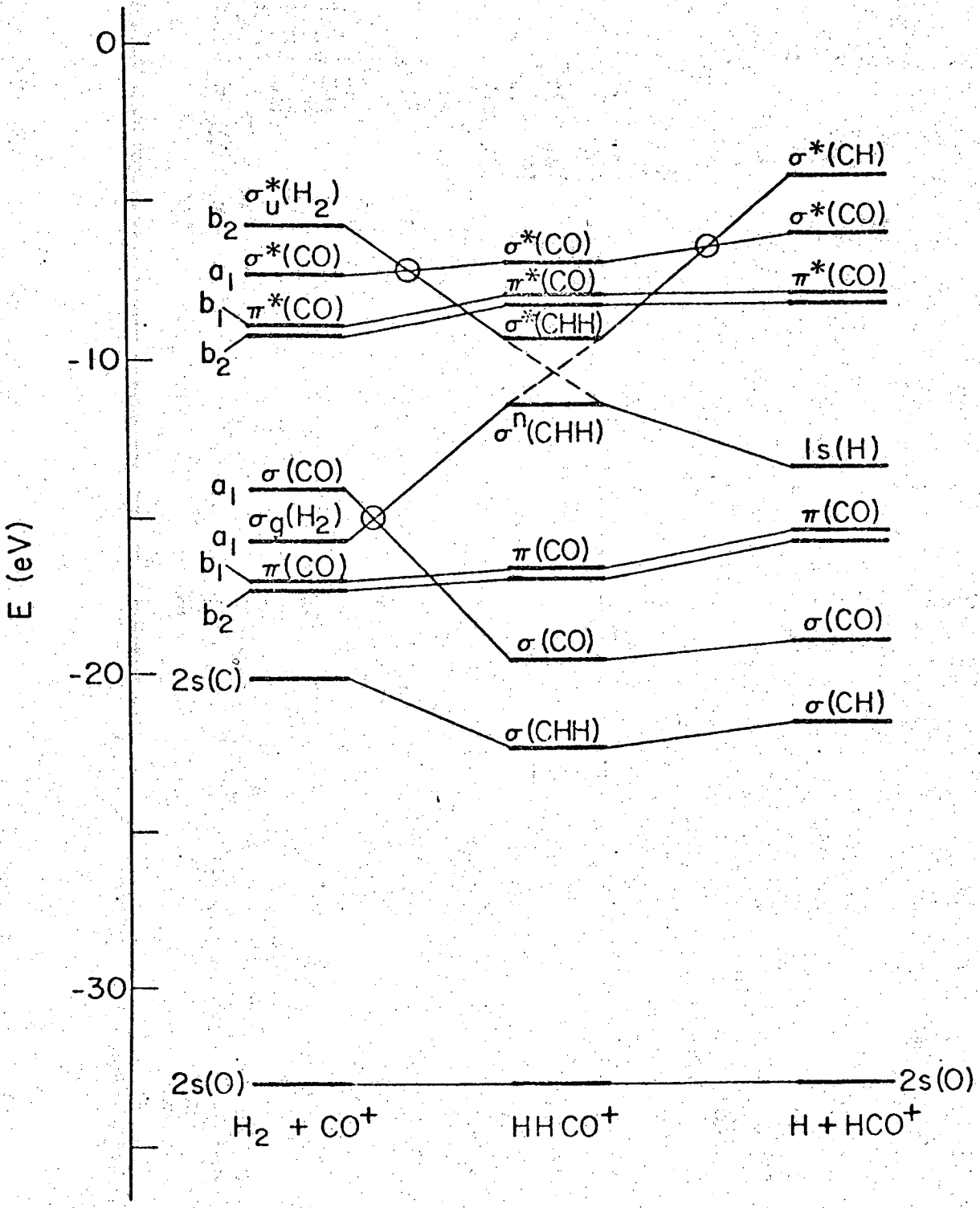


Fig. 6

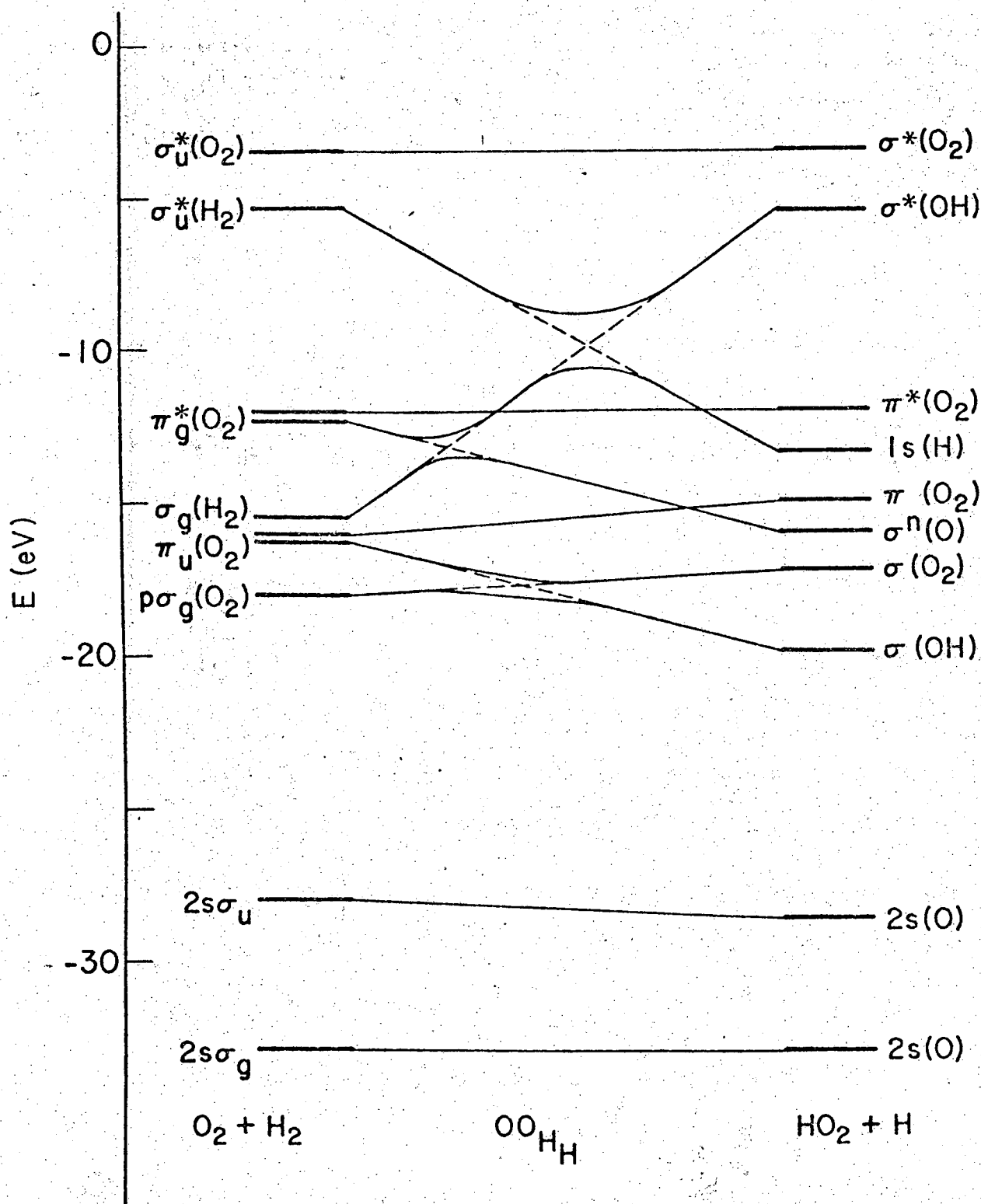


Fig. 8

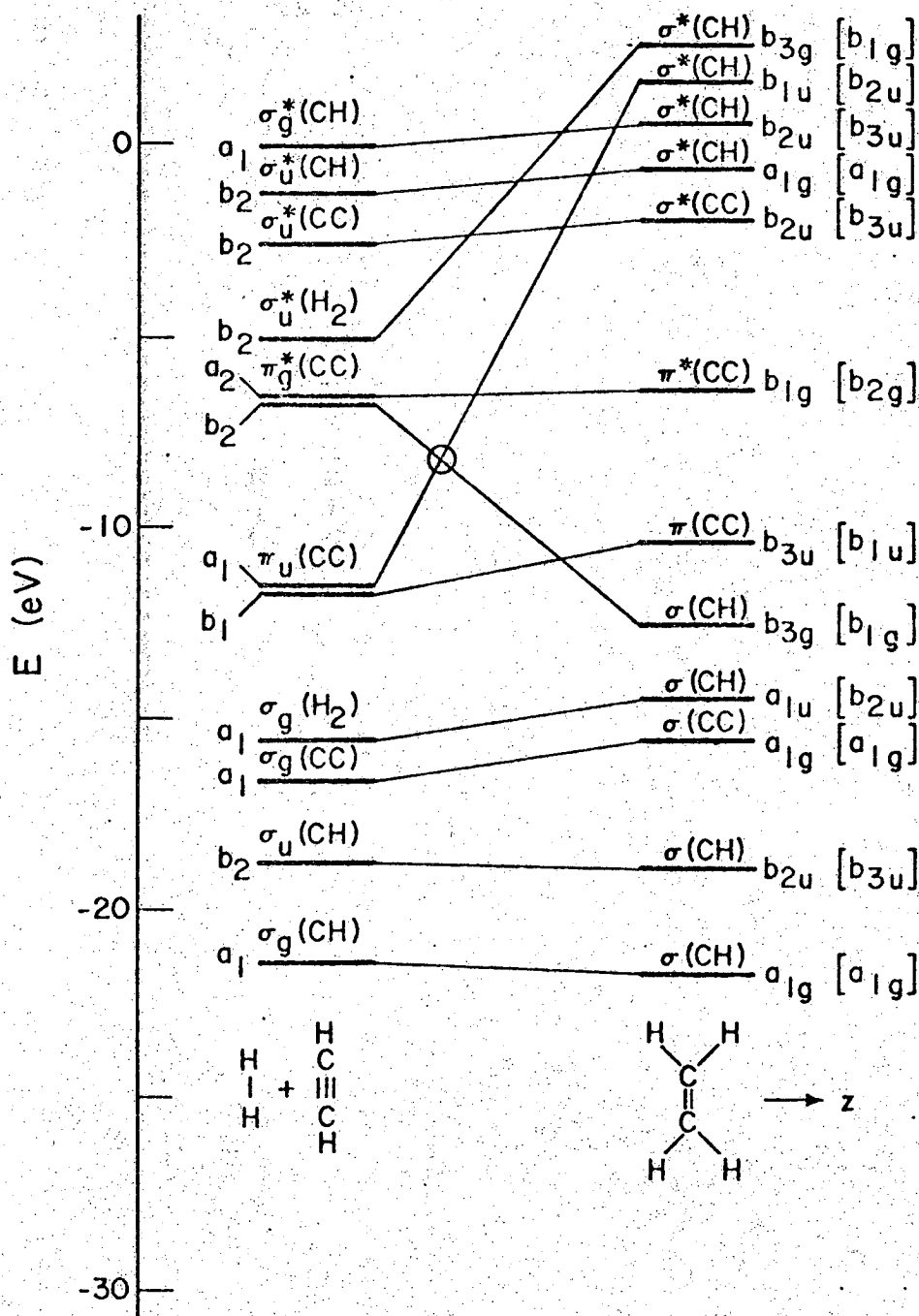


Fig. 9

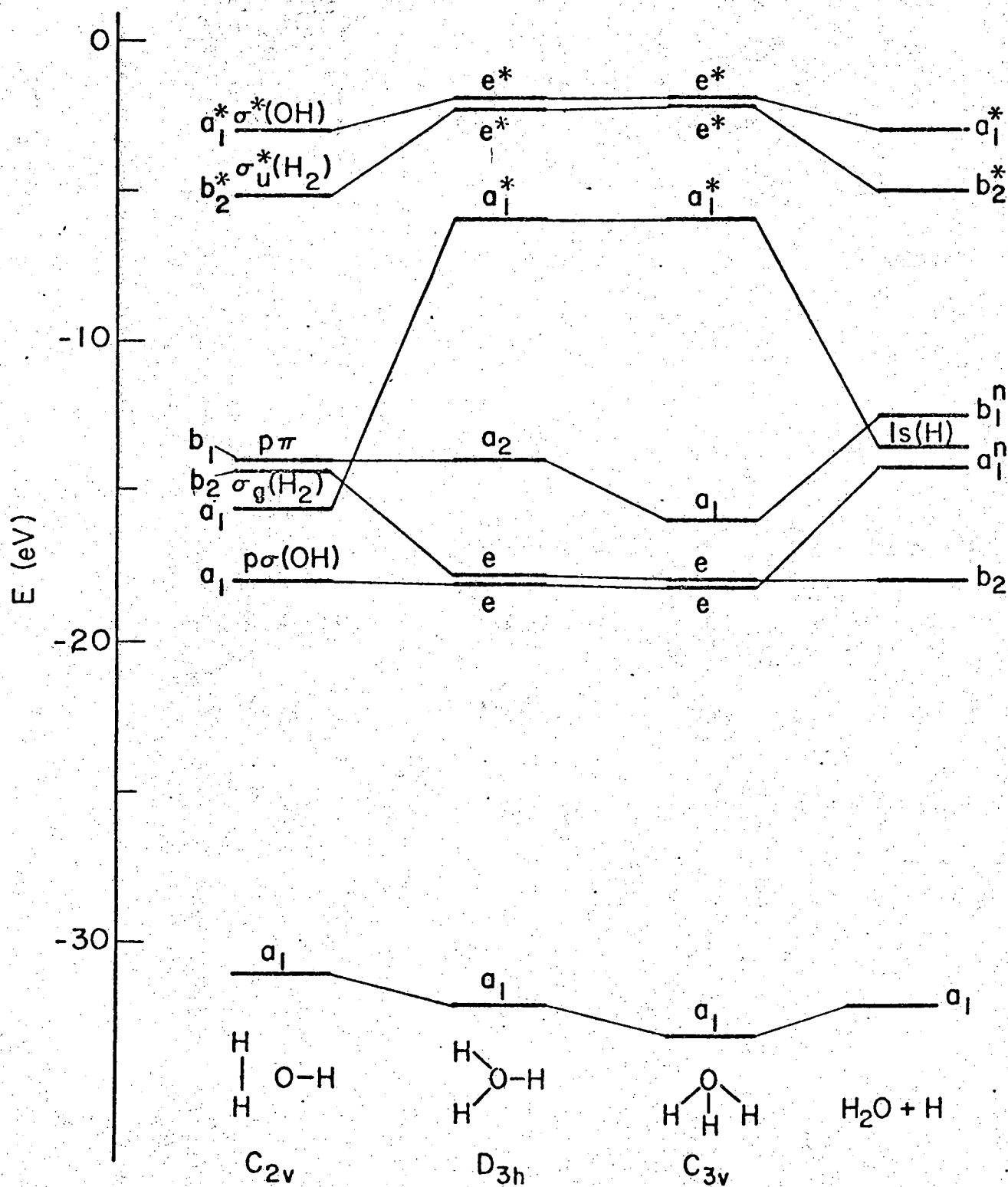


Fig. 10

LEGAL NOTICE

This report was prepared as an account of work sponsored by the United States Government. Neither the United States nor the United States Atomic Energy Commission, nor any of their employees, nor any of their contractors, subcontractors, or their employees, makes any warranty, express or implied, or assumes any legal liability or responsibility for the accuracy, completeness or usefulness of any information, apparatus, product or process disclosed, or represents that its use would not infringe privately owned rights.

TECHNICAL INFORMATION DIVISION
LAWRENCE RADIATION LABORATORY
UNIVERSITY OF CALIFORNIA
BERKELEY, CALIFORNIA 94720